

The QCD chiral transition temperature in a Dyson-Schwinger-equation context

M. Blank* and A. Krassnigg†

Institut für Physik, Karl-Franzens-Universität Graz, A-8010 Graz, Austria

(Dated: September 5, 2018)

We analyze the chiral phase transition with the help of the QCD gap equation. Various models for the effective interaction in rainbow truncation are contrasted with regard to the resulting chiral transition temperatures. In particular, we investigate possible systematic relations of the details of the effective interaction and the value of T_c . In addition, we quantify changes to the transition temperature beyond the rainbow truncation.

PACS numbers: 11.30.Rd, 12.38.Lg, 11.10.Wx

Keywords:

I. INTRODUCTION

The structure of the phase diagram of quantum chromodynamics (QCD) has recently received a lot of attention. Theoretical progress in various directions is well in line with past, present, and upcoming experimental programs e.g. at CERN SPS, RHIC, LHC, and FAIR. Among the key features of the phase diagram is the chiral phase transition at nonzero temperature and vanishing chemical potential. This transition has been and is studied extensively by various different approaches with an emphasis on the critical behavior of the order parameter as well as on the actual value of the transition temperature T_c . Lattice QCD calculations for example over the past years yielded T_c at temperatures between 145 and 200 MeV with a recent tendency towards a commonly found value [1–7]. In various model approaches in mean-field approximation and beyond one finds a range from 90 to 160 MeV, see e.g., [8] and references therein.

Although an understanding of the universal properties of QCD is of great importance, it is also rewarding to investigate the value of T_c which is not universal and can therefore be used to draw conclusions about specific details of the underlying dynamics of quarks and gluons. More precisely, specific models and their assumptions can be falsified in the approach presented here by a calculation of T_c in QCD.

II. FINITE-TEMPERATURE APPLICATIONS OF DYSON-SCHWINGER EQUATIONS

A nonperturbative continuum approach to QCD is provided by the Dyson-Schwinger equations (DSEs) [9, 10], which can be applied straight-forwardly also for finite temperature and chemical potential [11]. The DSEs are well-suited to study the properties of QCD's elementary degrees of freedom, quarks and gluons. In this framework, various aspects of chiral symmetry and its dynam-

ical breaking have been studied some time ago via the DSE of the quark propagator (also referred to as the “QCD gap equation”) at zero temperature (see, e.g. [12] and references therein) and in connection with the phase diagram of QCD (see, e.g. [11] and references therein). The same framework also allows the consistent and covariant study of bound-state, i.e. meson and baryon, properties. At zero temperature, a level of sophistication beyond simple QCD modeling has been reached (see e.g. [13–15] and references therein). At nonzero temperature and density, analogous investigations are complicated by the additional variables introduced in the Matsubara formalism. Nonetheless, investigations of meson masses at and beyond the phase transition at zero chemical potential [16–22] as well as certain aspects of the phase diagram [23–28] have been conducted at various but mostly simpler degrees of sophistication. In the present context, our focus is on DSE studies of the chiral phase transition in QCD at finite temperature and zero chemical potential.

It was shown some time ago that certain classes of models in the QCD gap equation in rainbow truncation yield a second-order phase transition with mean-field critical exponents [29, 30]. While the main emphasis of that investigation was the critical behavior and universality class of the phase transition, it also provided the corresponding values for T_c , which ranged between 120 and 174 MeV among the model interactions investigated. In somewhat different setups, using a separable interaction kernel in the gap equation [17, 19, 20, 31] or neglecting retardation effects [21], one obtains values in the range between 110 and 146 MeV.

The pointwise behavior of all these interactions as a function of the gluon momentum is rather different, although in all cases it was determined by adjusting the relevant parameters to meson phenomenology at zero temperature. Therefore, it is interesting to ask whether there is any simple relationship between the momentum dependence of the interaction and the value of T_c . Such a relationship could e.g. be analogous to that found recently in studies of meson properties using a particular form of model interaction with a one-parameter setup. There the value of the free parameter determines an effective range of the intermediate- and low-momentum parts of

*martina.blank@uni-graz.at

†andreas.krassnigg@uni-graz.at

the interaction. While ground-state properties of pseudoscalar and vector mesons were unaffected by variations in the model parameter, masses of excitations of any kind (orbital or radial) showed a strong and systematic dependence on the model parameter [14, 32–35] thus identifying excited-state properties as prime targets to study the particular details of the effective interaction in the DSE formalism, in particular in the nonperturbative regime. In an analogous fashion, the goal of the present work is to identify T_c as a quantity with the same capability. In particular, one can expect a calculation of T_c to impose even stronger restrictions on model parameters, beyond what is at hand at zero temperature.

The paper is organized as follows: Sec. III briefly sketches the quark DSE in QCD at finite temperature, Sec. IV compares the model interactions used herein, Sec. V outlines how we compute T_c and the critical exponents. The results are presented in Secs. VI and VII, the latter focusing on effects from corrections beyond rainbow truncation. Conclusions and an outlook are presented in Sec. VIII. All calculations are performed in Euclidean space.

III. QCD GAP EQUATION AT FINITE TEMPERATURE

We use the quark DSE to study the chiral phase transition of QCD. It is an inhomogeneous nonlinear integral equation for the dressed-quark propagator, whose inverse at $T = 0$ is of the form

$$S^{-1}(p) = i\gamma \cdot p A(p^2) + B(p^2), \quad (1)$$

where the four-vector p denotes the quark momentum and A and B are scalar functions of the momentum-squared. At nonzero temperature the presence of the heat bath implies an additional four vector, which leads to more structures in (1) [36]. In the Matsubara formalism one arrives at

$$S^{-1}(\vec{p}, \omega_k) = i\vec{\gamma} \cdot \vec{p} A(\vec{p}^2, \omega_k) + B(\vec{p}^2, \omega_k) + i\gamma_4 \omega_k C(\vec{p}^2, \omega_k) + \vec{\gamma} \cdot \vec{p} \gamma_4 \omega_k D(\vec{p}^2, \omega_k) \quad (2)$$

Now the four scalar functions (A, B, C, D) depend on the quark 3-momentum squared \vec{p}^2 and the quark's fermion Matsubara frequency $\omega_k = 2\pi T(k + 1/2)$, $k \in \mathbf{Z}$.

The QCD gap equation in pictorial form reads

$$\left(\text{diagram of } S(\vec{p}, \omega_k) \right)^{-1} = \left(\text{diagram of } S_0(\vec{p}, \omega_k) \right)^{-1} + \text{diagram of } S(\vec{q}, \omega_l) \text{ with gluon and quark-gluon vertex}, \quad (3)$$

where $S_0(\vec{p}, \omega_k)$ is the free quark propagator, $D_{\mu\nu}(\vec{p} - \vec{q}, \omega_k - \omega_l)$ the renormalized dressed gluon propagator and $\Gamma_\mu(\vec{p}, \omega_k; \vec{q}, \omega_l)$ the renormalized dressed quark-gluon vertex. Solving for $S(\vec{p}, \omega_k)$ one needs expressions for the quark-gluon vertex as well as the gluon propagator.

TABLE I: Parameter sets D and ω used for the different interactions MN [37], Eq. (10); AWW [38], Eq. (11); MT [39], Eq. (12); MR [40], Eq. (13); together with corresponding observables in $T = 0$ meson studies, where available. Numbers are in GeV except for D (GeV²) and the chiral condensate, whose dimension is given explicitly.

Model	ω	D	$-\langle \bar{q}q \rangle_0$	m_π	m_ρ
MN		0.5618	(.115 GeV) ³	0.14	0.77
AWW1	0.3	1.47	(.245 GeV) ³	0.135	0.745
AWW2	0.4	1.152	(.246 GeV) ³	0.135	0.748
AWW3	0.5	1.0	(.251 GeV) ³	0.137	0.758
MT1	0.3	1.24	(.243 GeV) ³	0.139	0.747
MT2	0.4	0.93	(.242 GeV) ³	0.139	0.743
MT3	0.5	0.744	(.239 GeV) ³	0.141	0.724
MR1	0.3	0.78	(.241 GeV) ³	0.139	
MR2	0.4	0.78	(.250 GeV) ³	0.139	
MR3	0.5	0.78	(.255 GeV) ³	0.139	

These can in principle be obtained from their own DSEs self-consistently, which is clearly beyond the scope of the present study. Instead we use various model Ansätze in a rainbow truncation of the gap equation, as specified below. Defining the gluon four momentum as $(\vec{k}, \Omega) := (\vec{p} - \vec{q}, \omega_k - \omega_l)$, the second term on the right-hand side of (3), the quark self energy $\Sigma(\vec{p}, \omega_k)$, is given by

$$\Sigma(\vec{p}, \omega_k) = T \sum_{l=-\infty}^{\infty} \int \frac{d^3 q}{(2\pi)^3} \frac{4}{3} g^2 D_{\mu\nu}(\vec{k}, \Omega) \times \gamma_\nu S(\vec{q}, \omega_l) \Gamma_\mu(\vec{p}, \omega_k; \vec{q}, \omega_l). \quad (4)$$

The gap equation is subject to the renormalization condition that for a renormalization scale ζ and $\vec{p}^2 + \omega_0^2 = \zeta^2$

$$S^{-1}(\vec{p}, \omega_0) = i\vec{\gamma} \cdot \vec{p} + i\gamma_4 \omega_0 + m(\zeta). \quad (6)$$

Note that this condition does not contain a term $\vec{\gamma} \cdot \vec{p} \gamma_4 \omega_k$, i.e., the scalar function $D(\vec{p}^2, \omega_k)$ will be power-law suppressed in the ultra-violet [11].

In the following, unless otherwise noted, we use the rainbow-truncated gap equation by setting $\Gamma_\mu(\vec{p}, \omega_k; \vec{q}, \omega_l) = \gamma_\mu$. The finite- T expression for the renormalized dressed gluon propagator in Landau gauge reads [11, 41]

$$g^2 D_{\mu\nu}(\vec{k}, \Omega) = P_{\mu\nu}^L(\vec{k}, \Omega) \mathcal{G}(\vec{k}, \Omega; m_g) + P_{\mu\nu}^T(\vec{k}, \Omega) \mathcal{G}(\vec{k}, \Omega; 0), \quad (7)$$

$$P_{\mu\nu}^T(\vec{k}, \Omega) = \begin{cases} 0, & \mu \text{ and/or } \nu = 4 \\ \delta_{ij} - \frac{k_i k_j}{\vec{k}^2}, & \mu, \nu = i, j = 1, 2, 3 \end{cases}, \quad (8)$$

$$P_{\mu\nu}^L(\vec{k}, \Omega) = \delta_{\mu\nu} - \frac{k_\mu k_\nu}{\vec{k}^2 + \Omega^2} - P_{\mu\nu}^T, \quad (9)$$

where m_g is a Debye mass [42] and \mathcal{G} is an effective interaction detailed below.

IV. INTERACTION MODELS

At zero temperature covariant bound-state equations have been used to study the properties of hadrons in various particular setups in order to gain insight regarding the properties of the underlying fundamental Green functions of QCD from a phenomenological point of view. More concretely, for the case of mesons the Bethe-Salpeter-Equation in ladder truncation together with the gap equation in rainbow truncation has been employed using many different Ansätze for the quark-gluon interaction to investigate various meson properties, see [14] and references therein. In that process, different effective interactions have been tested by employing model-independent constraints for the interaction and fixing the remaining (in our case either one or two) parameters and a current-quark mass to phenomenological and experimental numbers such as the chiral condensate, the pion mass, and the pion decay constant.

In the present work we investigate four different functional forms of the interaction, referred to in the following by MN (Munczek-Nemirovsky [37]), AWW (Alkofer-Watson-Weigel [38]), MT (Maris-Tandy [39]), and MR (Maris-Roberts [40]), in order of complexity. The zero-temperature effective interaction can be straightforwardly used at finite temperature by insertion in Eq. (7). Via $s := \vec{k}^2 + \Omega^2 + m_g^2$ one gets

$$\mathcal{G}(\vec{k}, \Omega; m_g) =$$

$$\text{MN} : = D \frac{4\pi^3}{T} \delta^3(\vec{k}) \delta_{k-l,0} \quad (10)$$

$$\text{AWW} : = D \frac{4\pi^2}{\omega^6} s e^{-s/\omega^2} \quad (11)$$

$$\text{MT} : = D \frac{4\pi^2}{\omega^6} s e^{-s/\omega^2} + \mathcal{F}_{UV}(s) \quad (12)$$

$$\text{MR} : = D \left(\frac{4\pi^3}{T} \delta^3(\vec{k}) \delta_{k-l,0} + \frac{4\pi^2}{\omega^6} s e^{-s/\omega^2} \right) + \mathcal{F}_{UV}(s), \quad (13)$$

$$\mathcal{F}_{UV}(s) : = \frac{4\pi \gamma_m \pi \mathcal{F}(s)}{1/2 \ln[\tau + (1 + s/\Lambda_{\text{QCD}}^2)^2]}$$

As given in [39], $\mathcal{F}(s) = [1 - \exp(-s/[4m_t^2])]/s$, $m_t = 0.5 \text{ GeV}$, $\tau = e^2 - 1$, $N_f = 4$, $\Lambda_{\text{QCD}}^{N_f=4} = 0.234 \text{ GeV}$, and $\gamma_m = 12/(33 - 2N_f)$. At $T = 0$ all of these Ansätze provide the correct amount of dynamical chiral symmetry breaking as well as quark confinement via the absence of a Lehmann representation for the dressed quark propagator. In addition, MT and MR produce the correct perturbative limit of the QCD running coupling, i.e. they preserve the one-loop renormalization-group behavior of QCD for solutions of the quark DSE. Thus, for MT and MR, a renormalization procedure is needed in the gap equation, which we implement following Refs. [18, 40], where the necessary details can be found.

Here, for the interactions in Eqs. (11), (12), and (13), we investigate different parameter sets (i.e., values of D

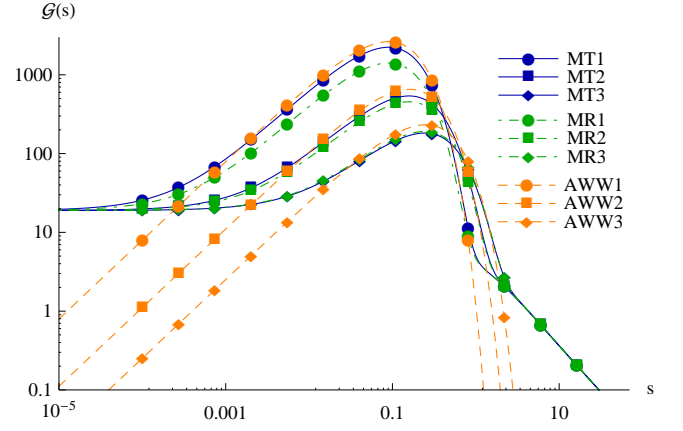


FIG. 1: (Color online) Plot of the different forms for the effective interaction used in this work as simple functions of a momentum squared s . The corresponding parameters can be found in Tab. I. Note the different behavior of the interactions on all momentum ranges. In particular, the reader should keep in mind that the δ -function present in MR, Eq. (13) is invisible in the double-logarithmic presentation as well as the MN interaction, Eq. (10), which is zero for $s \neq 0$.

and ω) in analogy to the corresponding bound-state studies at $T = 0$. Table I lists these sets of parameters together with the respective results for relevant $T = 0$ observables. Once D and ω have been fitted to the chiral condensate, one remains with a u/d current-quark mass to be chosen in order to calculate properties of light mesons. For each set the light quark mass has been adjusted to fit m_π ; m_ρ is listed for a first corresponding result without fixing any further parameters. Since our study will remain in the chiral limit, the meson masses are included only to complete the justification of the model parameters.

For easy reference and an instructive comparison, the effective interaction for all parameter sets is plotted in Fig. 1. Differences are clearly visible in the UV regime. In the IR one has to keep in mind that the δ -function present in the MR interaction, Eq. (13) is not shown here due to the double-logarithmic presentation as well as the MN interaction, Eq. (10), which is zero for $s \neq 0$. The intermediate momentum region is dominated by the Gaussian peak whose position and width are characterized by the parameter ω and whose overall strength is D .

The reader may ask whether there is any relation between D and ω that could simplify the parameterization. Indeed, inspection of Tab. I shows that for the MT interaction the product ωD is constant over the range of values for ω used here, when one aims at a given value of the chiral condensate. In addition, without changing the value of the u/d current-quark mass, also m_π (and approximately also m_ρ) are unchanged on this domain, which can be used to motivate a redefinition of the parameters [43]. As already mentioned in Sec. II, one can interpret this pattern with regard to ω such that this

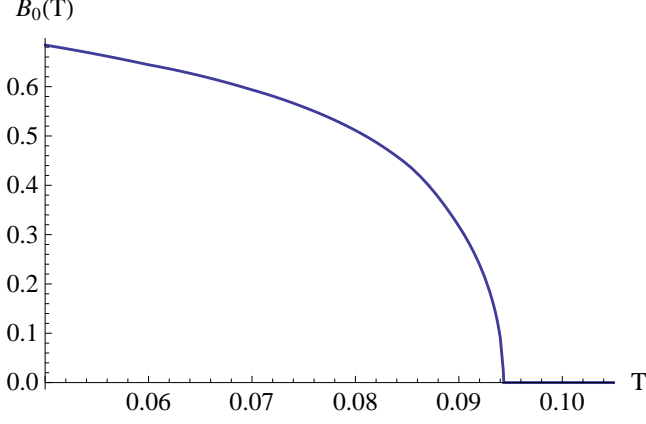


FIG. 2: (Color online) Plot of the order parameter B_0 vs. temperature T , shown exemplarily for model MT2.

parameter represents an inverse effective range of the interaction, a dependence on which should be less prominent in ground-state properties than for excited states. However, for the other interaction types, such a simple relation among the parameters does not exist and so we keep the interactions in their present form.

V. CHIRAL PHASE TRANSITION

With all ingredients of the QCD gap equation at hand one can obtain a solution numerically and study the chiral phase transition temperature T_c as well as the nature of the transition. The corresponding order parameter is the chiral condensate. Equivalently, we use $B_0 := B(0, \omega_0)$, since it is easier to access and can be calculated more accurately. A typical behavior of the order parameter for a chiral-limit solution is shown in Fig. 2 and indicates a second order phase transition. Indeed as mentioned earlier, it has been found previously that the rainbow-truncated quark DSE generally yields a second order chiral phase transition with mean-field critical exponents [29, 30]. We have confirmed this behavior for all interactions considered here and thus enlarged the set of interaction types it had been shown for by MT and AWW. The following account of our procedure includes the discussion of critical exponents mainly for completeness, but also, since as described below, T_c can be extracted more accurately this way. In the case of a second order phase transition, the order parameter $B_0(t, h)$ obeys the scaling laws

$$B_0(t, h) \propto (-t)^\beta \Big|_{h=0} \quad t \rightarrow 0^- \quad \text{and} \quad (14)$$

$$B_0(t, h) \propto h^{1/\delta} \Big|_{t=0} \quad h \rightarrow 0^+. \quad (15)$$

Here, $t = \frac{T}{T_c} - 1$ is the reduced temperature and $h = \frac{m}{T}$ the reduced mass, a measure for the explicit breaking of chiral symmetry by a non-vanishing current quark mass

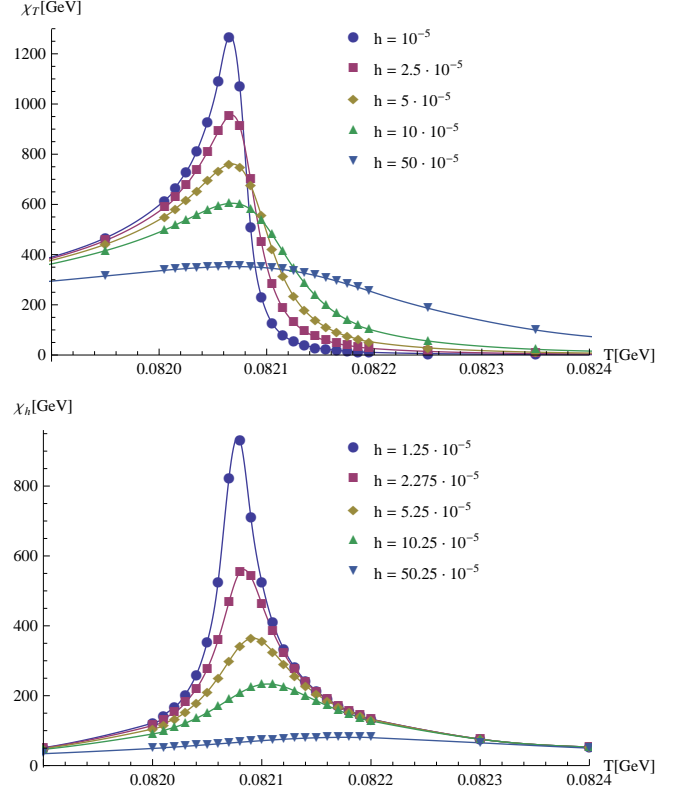


FIG. 3: (Color online) Chiral susceptibilities $\chi_T(T)$ (upper panel) and $\chi_h(T)$ (lower panel) for the MT1 model plotted versus temperature T for various values of h . The curves between the data points were obtained by interpolation using cubic splines.

m . β and δ are the critical exponents of the phase transition.

Although it is straightforward to use Eqs. (14)-(15) to obtain β and δ , this procedure requires to solve the gap equation at $h = 0$ or $T = T_c$. This is numerically difficult, such that a direct evaluation does not allow fits to extract T_c with the necessary precision and reliably observe scaling. Therefore we exploit further scaling relations and use chiral susceptibilities for our analysis. They are defined by

$$\chi_T := -T_c \frac{\partial B_0(T, h)}{\partial T} \Big|_{h \text{ fixed}}, \quad \text{and} \quad (16)$$

$$\chi_h := \frac{\partial B_0(T, h)}{\partial h} \Big|_{T \text{ fixed}}. \quad (17)$$

The maxima of these quantities for nonvanishing h are referred to as pseudocritical points, χ_T^{pc} and χ_h^{pc} , respectively. The corresponding pseudocritical temperatures are denoted by T_T^{pc} and T_h^{pc} . They are obtained as the maxima of the chiral susceptibilities with respect to temperature, as depicted in Fig. 3.

The pseudocritical points χ_T^{pc} and χ_h^{pc} also obey scaling laws. Their behavior for $T \sim T_c$ and $h \sim 0$ is described

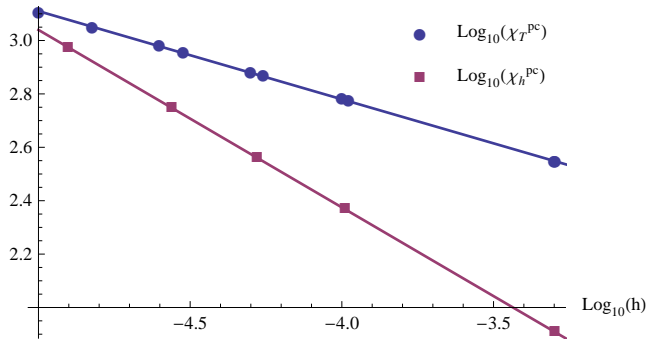


FIG. 4: (Color online) Peak heights of the chiral susceptibilities χ_T^{pc} and χ_h^{pc} plotted versus the reduced mass h on log-log scale, for the MT1 model. The lines are linear fits through the calculated points which are used to obtain the critical exponents according to Eqs. (18) - (19).

by

$$\chi_T^{pc} \propto h^{-1+1/\delta}, \quad (18)$$

$$\chi_h^{pc} \propto h^{\frac{1}{\beta\delta}(1-\beta)}. \quad (19)$$

Following [44] we use these scaling relations to obtain β , δ , and T_c for the all models and parameter sets given in Tab. I, as illustrated in Fig. 4.

VI. RESULTS AND DISCUSSION

As already mentioned above, all interactions yield a second order phase transition with mean-field critical exponents, regardless of the strength of the interaction, its range, or its pointwise behavior in any particular momentum range. In particular, the presence of the δ -function term does not make a difference in this respect. Another general observation is the fact that the function $D(\vec{p}^2, \omega_k)$ in Eq. (2) is identically zero for all interactions in rainbow truncation.

The values obtained for the chiral transition temperature T_c , however, are rather different among the various interactions. In the following we will argue how this feature can be exploited to discern various forms within a given truncation. The results for T_c are summarized in Tab. II for the four interactions on a range of model parameters well-used in meson phenomenology.

The MN interaction has to be treated somewhat separately, since the only free parameter in this case is D whose choice completely determines \mathcal{G} . In terms of plain numbers it is interesting to see that MN yields the highest value for T_c , followed by MR. AWW and MT give the smallest numbers.

For a given interaction, T_c increases with ω , which is illustrated in panel (a) of Fig. 5. A straight-forward interpretation of this observation goes back to ω representing

TABLE II: Results for the transition temperature T_c rounded to MeV for the interactions and parameter sets defined in Tab. I.

ω [GeV]	N/A	0.3	0.4	0.5
Model	MN			
T_c	169			
Model	AWW1	AWW2	AWW3	
T_c	82	94	101	
Model	MT1	MT2	MT3	
T_c	82	94	96	
Model	MR1	MR2	MR3	
T_c	120	133	144	

an inverse effective range of the interaction. In this picture, T_c is higher for an interaction, for which this range is smaller, i.e. the major strength in the interaction comes from a region defined by the larger momentum scale ω . However, this effect is obviously minor compared to the differences with regard to the form of the interaction, in particular the appearance of the δ -function term.

To further illustrate the details of the differences between the various forms for the interaction as well as to highlight their characteristic features, we plot T_c as a function of three more specific properties of each model, namely ωD in panel (b), D in panel (c), and the chiral condensate in panel (d). While the attempt to quantitatively correlate T_c globally (i.e. across the different interactions) to any of these fails, a clear structure is visible. Throughout all panels of Fig. 5 the AWW and MT results are rather close together, but clearly separate from MR, which again is clearly separate from MN.

Both ωD and D investigated in the two middle panels have been interpreted as an “integrated strength” of the interaction. In fact, the latter is proportional to the integral over d^4q of the interaction at zero temperature for all interactions investigated here, if one leaves out the UV part \mathcal{F}_{UV} in Eqs. (12) and (13). Fig. 5 in panel (c) clearly shows that there is no overall simple dependence of T_c on D . In the MT interaction, a constant value for ωD leads to (almost) unchanged masses and decay constants for ground-state pseudoscalar and vector mesons, for which reason ωD can be termed “integrated strength” in this case instead of D . Again, Fig. 5 in panel (b) indicates no simple dependence of T_c on ωD . In both cases, the absence of a simple relation is exemplified already by the fact that three points with the same ωD , the characteristic feature for MT, in Fig. 5 (b) and three points with the same D , the characteristic feature for MR, in Fig. 5 (c) each correspond to three different values of T_c .

Finally, in Fig. 5 (d) we plot T_c as a function of an order parameter of chiral symmetry breaking, the chiral condensate, evaluated at $T = 0$. In a very simple picture, one could argue that, given a certain form of the dependence of the order parameter on the temperature (see, e.g. Fig. 2), an enlargement of the value of the order

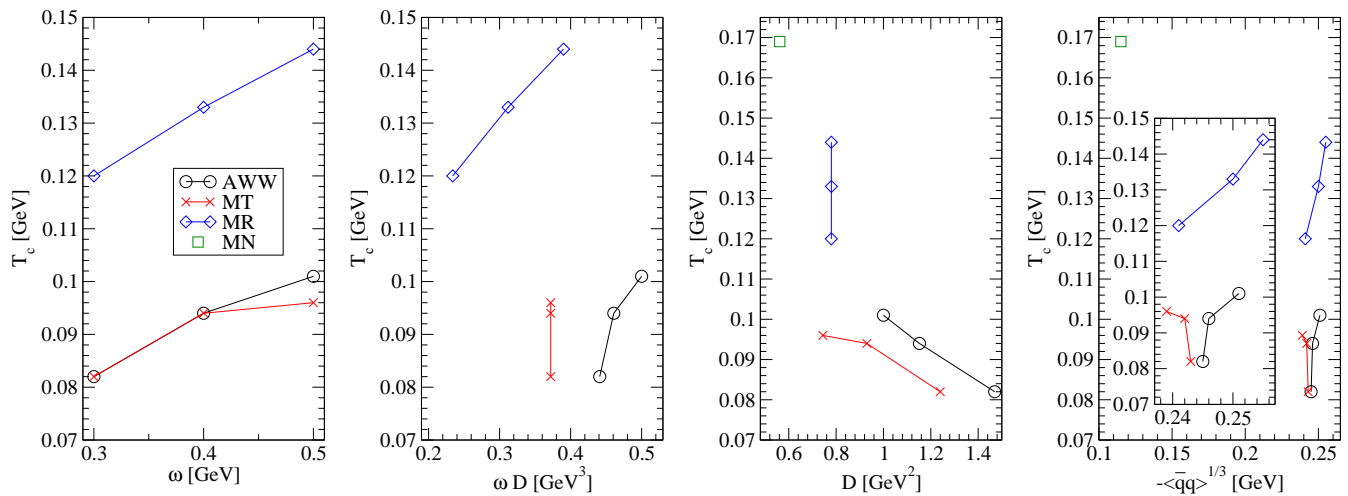


FIG. 5: (Color online) From left to right, the four panels show the results for T_c as a function of: ω , leftmost panel (a); ωD , left-middle panel (b); D , right-middle panel (c); and the chiral condensate, rightmost panel (d). The different colors and symbols on the lines denote the corresponding interactions, namely: black (circles) – AWW; red (X) – MT; and blue (diamonds) – MR. The result for MN (single green square) is only shown in panels (c) and (d), since it does not have a value of ω associated with it. The insert in panel (d) enlarges the region of interest for the ω -dependent interactions.

parameter at $T = 0$ would naturally lead to an increase in T_c . However, panel (d) clearly shows that the interactions used in our setup are not that simple.

Overall, these observations lead to the important possibility to establish distinct ranges of values for T_c accessible for each type of interaction, which has the potential to rule out certain forms in a given truncation. We note here that various effects need to be taken into account beyond the simple setup presently used; we will attempt to quantify some of them below. At this point, however, we can still try to attribute the clear differences apparent from all panels in Fig. 5 to the structure of the interaction. The object of interest in this respect is the appearance and relative strength of the δ -function term in \mathcal{G} , Eqs. (10) – (13): In the AWW and MT interactions, Eqs. (11) and (12), there is no such term. In the MR interaction, Eq. (13), it carries half the strength of the coupling in the sense of the integral $\int d^4q \mathcal{G} \sim D$ described above. In the MN interaction, Eq. (10), it is the only term and obviously represents all of the interaction's strength. From this, one can say that a less pronounced δ -function term in the interaction will lead to lower values of T_c .

VII. BEYOND RAINBOW TRUNCATION

While the rainbow truncation of the gap equation provides a simple setup for computations, one has to keep in mind that the necessary corrections in any given circumstance may change its results considerably. Therefore we discuss here some of the most important effects from which a change, in particular to the critical temperature, is to be expected.

From a phenomenological point of view one can try to quantify the contribution of the rainbow-truncated gap equation to the full (untruncated) result. Such an attempt has been made for meson properties at zero temperature in [43] and has been extended to the baryon sector and exemplified for several hadronic observables in [45]. The idea is to change the values of the available model parameters such that the resulting hadron properties, e.g. the rho-meson mass, are deliberately overestimated by the rainbow-ladder truncation result. In this way one expects corrections beyond this truncation to bring it to the experimental value.

While we do not want to discuss the particular assumptions made in [43, 45], the effect described there is relevant for our present study, since we start with model parameters fixed to meson phenomenology at zero temperature. To get a first estimate of the effects from a change of parameters at $T = 0$ on T_c , we simply adapt the two parameter sets referred to as “A” (which corresponds to our MT2 parameter set) and “B” (which has increased strength in the interaction to overestimate the rho-meson mass as discussed above) in Ref. [45] and add T_c to the Tab. I given there. In this table, a systematic ratio of ≈ 0.74 is found for value in A divided by value in B for several hadron properties (e.g. m_ρ , f_π , m_N , m_Δ , etc.). Our values for T_c in this respect are 94 MeV for set A and 129 MeV for set B, which produces a ratio of 0.73 and thus fits perfectly into the picture.

For the present discussion here the relevant point is that parameter changes inferred from the phenomenological estimation of corrections expected beyond rainbow-ladder truncation are in agreement with investigations at zero temperature. In particular, one obtains an increase of T_c by about one third, depending on the details of the

corrections assumed.

A different investigation by D. Blaschke, D. Horvatić, and D. Klabučar regarding the role of the Polyakov loop in an analogous, separable setup of the quark DSE at finite temperature indicates that the inclusion of a Polyakov-loop potential shifts T_c up by ≈ 70 MeV [46]. This is also observed in other approaches such as Polyakov-quark-meson studies or Polyakov-Nambu–Jona-Lasinio-type models, see e.g. [47] and references therein.

Finally, we briefly quantify corrections from inclusion of more structure in the quark self-energy, in particular in the dressed quark-gluon vertex. Ideally, one would together with the gap equation also solve the Dyson-Schwinger equations for the gluon propagator and the quark-gluon vertex—the two unknown ingredients in the DSE for the quark propagator—as self-consistently as possible at any given finite temperature. Such investigations have already been started at $T = 0$ (see e.g. [48] and references therein) and represent a natural and very promising, but at the same time rather involved path for future extensions of the present study.

In a more immediate way, one can identify corrections to rainbow truncation from the terms in the quark-gluon-vertex DSE and attempt to incorporate these into the gap equation. Pion-loop contributions have been investigated at $T = 0$ in [49]. Ref. [50] reports preliminary results of an analogous study at finite temperature, which indicate a reduction of T_c of about 5% upon the inclusion of pion-loop, but not scalar-meson-loop corrections in the quark self energy and no change of the (mean field) critical exponents.

Another effect, coming from the combination of two other vertex corrections, can be estimated by an extension of a simple MN-study of quark and meson properties presented in [51] to finite temperature. This is a straightforward procedure, which has many aspects and will be investigated in full detail elsewhere [52]. For the moment we note that a first estimate of shifts in T_c are of the order of 15%. Another interesting observation is that in the course of dressing the bare quark-gluon vertex one can arrive at results with the possibility for solutions of the gap equation with $D(\vec{p}^2, \omega_k) \neq 0$.

To conclude this section, we remark that corrections to the rainbow truncation of the quark DSE should not be viewed as corrections to a mean-field approximation; corrections in the quark self energy in our present calculations happen at the level of the structure of the quark-gluon vertex. We would also like to emphasize that, although not demonstrated explicitly here, for finite current-quark masses we obtain a smooth crossover instead of a second-order phase transition.

VIII. CONCLUSIONS AND OUTLOOK

We have investigated the impact of various forms of an effective quark-gluon interaction in the rainbow-truncated quark DSE in QCD at finite temperature on the critical temperature of the chiral phase transition. The established mean-field behavior of this transition in the present truncation is confirmed throughout. Regarding non-universal aspects of the transition, it is apparent that there is no simple overall relationship between the distribution of the infrared strength of the interaction and the critical temperature, although 1) a trend can be extracted identifying the part of the interaction strength carried by a δ -function term in some of the models as a qualitatively distinctive parameter, and 2) within the various models simple relations of T_c and relevant model parameters do exist.

Changes of T_c due to various corrections to the present truncation are quantified and put into context. In addition to effects already described in the literature we estimate particular types of corrections in the present work using phenomenological arguments on one hand as well as a simple model-extension of the quark-gluon vertex on the other hand. Altogether, the various corrections put our results in a consistent perspective with regard to the results for T_c obtained in other approaches.

Furthermore, the present results clearly show that the chiral transition temperature is an excellent candidate for detailed studies of various aspects of the strong interaction. In particular it distinctively relates to both assumptions about as well as particular and detailed properties of the effective interaction between quarks and gluons in the DSE setup. Further studies beyond the present investigation will shed more light on this relationship as well as on how the mean-field behavior of the chiral phase transition may change beyond the current truncation.

Acknowledgments

The authors would like to acknowledge valuable discussions with R. Alkofer, G. Eichmann, D. Horvatić, D. Klabučar, and B.-J. Schaefer. A.K. would like to thank his colleagues at the Institute for Theoretical Physics of the University of Zagreb for their hospitality during the initial phase of this work. This work was supported by the Austrian Science Fund *FWF* under project no. P20496-N16, the Austrian Research Association *ÖFG* under MOEL stipend no. 248, and is performed in association with and supported in part by the *FWF* doctoral program no. W1203-N08.

-
- [1] Y. Aoki, Z. Fodor, S. D. Katz, and K. K. Szabo, Phys. Lett. B **643**, 46 (2006).
 - [2] C. Bernard et al. (MILC), Phys. Rev. D **71**, 034504

(2005).

- [3] M. Cheng et al., Phys. Rev. D **74**, 054507 (2006).
- [4] A. Bazavov et al., Phys. Rev. D **80**, 014504 (2009).

- [5] Y. Aoki, G. Endrodi, Z. Fodor, S. Katz, and K. Szabo, *Nature* **443**, 675 (2006).
- [6] Y. Aoki, S. Borsanyi, S. Durr, Z. Fodor, S. D. Katz, et al., *JHEP* **0906**, 088 (2009).
- [7] M. Cheng, N. Christ, S. Datta, J. van der Heide, C. Jung, et al., *Phys.Rev.D* **77**, 014511 (2008).
- [8] B.-J. Schaefer and J. Wambach, *Nucl. Phys. A* **757**, 479 (2005).
- [9] C. S. Fischer, *J. Phys. G* **32**, R253 (2006).
- [10] C. D. Roberts, M. S. Bhagwat, A. Holl, and S. V. Wright, *Eur. Phys. J. Special Topics* **140**, 53 (2007).
- [11] C. D. Roberts and S. M. Schmidt, *Prog. Part. Nucl. Phys.* **45**, S1 (2000).
- [12] P. Maris and C. D. Roberts, *Int. J. Mod. Phys. E* **12**, 297 (2003).
- [13] G. Eichmann, A. Krassnigg, M. Schwinzerl, and R. Alkofer, *Annals Phys.* **323**, 2505 (2008).
- [14] A. Krassnigg, *Phys. Rev. D* **80**, 114010 (2009).
- [15] G. Eichmann, R. Alkofer, A. Krassnigg, and D. Nicmorus, arXiv:0912.2246.
- [16] D. Horvatic, D. Klabucar, and A. E. Radzhabov, *Phys. Rev. D* **76**, 096009 (2007).
- [17] D. Horvatic, D. Blaschke, D. Klabucar, and A. E. Radzhabov, *Phys. Part. Nucl.* **39**, 1033 (2008).
- [18] P. Maris, C. D. Roberts, S. M. Schmidt, and P. C. Tandy, *Phys. Rev. C* **63**, 025202 (2001).
- [19] D. Blaschke, G. Bureau, Y. L. Kalinovsky, P. Maris, and P. C. Tandy, *Int. J. Mod. Phys. A* **16**, 2267 (2001).
- [20] D. Blaschke, Y. L. Kalinovsky, A. E. Radzhabov, and M. K. Volkov, *Phys. Part. Nucl. Lett.* **3**, 327 (2006).
- [21] R. Alkofer, P. A. Amundsen, and K. Langfeld, *Z. Phys. C* **42**, 199 (1989).
- [22] D. B. Blaschke, G. R. G. Bureau, M. A. Ivanov, Y. L. Kalinovsky, and P. C. Tandy, arXiv:hep-ph/0002047.
- [23] P. Maris, C. D. Roberts, and S. M. Schmidt, *Phys. Rev. C* **57**, 2821 (1998).
- [24] D. Blaschke and P. C. Tandy, arXiv:nucl-th/9905067.
- [25] D. Nickel, J. Wambach, and R. Alkofer, *Phys. Rev. D* **73**, 114028 (2006).
- [26] D. Nickel, R. Alkofer, and J. Wambach, *Phys. Rev. D* **74**, 114015 (2006).
- [27] H. Chen et al., *Phys. Rev. D* **78**, 116015 (2008).
- [28] T. Klahn, C. D. Roberts, L. Chang, H. Chen, and Y.-X. Liu, arXiv:0911.0654.
- [29] A. Holl, P. Maris, and C. D. Roberts, *Phys. Rev. C* **59**, 1751 (1999).
- [30] P. Maris, arXiv:nucl-th/9908069.
- [31] D. Blaschke, D. Horvatic, D. Klabucar, and A. E. Radzhabov, arXiv:hep-ph/0703188.
- [32] A. Holl, A. Krassnigg, and C. D. Roberts, *Phys. Rev. C* **70**, 042203(R) (2004).
- [33] A. Holl, A. Krassnigg, P. Maris, C. D. Roberts, and S. V. Wright, *Phys. Rev. C* **71**, 065204 (2005).
- [34] A. Krassnigg, *PoS Confinement* **8**, 75 (2009).
- [35] A. Holl, A. Krassnigg, C. D. Roberts, and S. V. Wright, *Int. J. Mod. Phys. A* **20**, 1778 (2005).
- [36] O. K. Kalashnikov, *JETP Lett.* **41**, 582 (1985).
- [37] H. J. Munczek and A. M. Nemirovsky, *Phys. Rev. D* **28**, 181 (1983).
- [38] R. Alkofer, P. Watson, and H. Weigel, *Phys. Rev. D* **65**, 094026 (2002).
- [39] P. Maris and P. C. Tandy, *Phys. Rev. C* **60**, 055214 (1999).
- [40] P. Maris and C. D. Roberts, *Phys. Rev. C* **56**, 3369 (1997).
- [41] J. I. Kapusta, *Finite Temperature Field Theory* (Cambridge University Press, 1989).
- [42] A. Bender, D. Blaschke, Y. Kalinovsky, and C. D. Roberts, *Phys. Rev. Lett.* **77**, 3724 (1996).
- [43] G. Eichmann, R. Alkofer, I. C. Cloet, A. Krassnigg, and C. D. Roberts, *Phys. Rev. C* **77**, 042202(R) (2008).
- [44] D. Blaschke, A. Holl, C. D. Roberts, and S. M. Schmidt, *Phys. Rev. C* **58**, 1758 (1998).
- [45] D. Nicmorus, G. Eichmann, A. Krassnigg, and R. Alkofer, *Phys. Rev. D* **80**, 054028 (2009).
- [46] D. Horvatic, private communication.
- [47] B.-J. Schaefer, J. M. Pawlowski, and J. Wambach, *Phys.Rev. D* **76**, 074023 (2007).
- [48] R. Alkofer, C. S. Fischer, F. J. Llanes-Estrada, and K. Schwenzer, *Annals Phys.* **324**, 106 (2009).
- [49] C. S. Fischer, D. Nickel, and J. Wambach, *Phys. Rev. D* **76**, 094009 (2007).
- [50] J. A. Mueller and C. S. Fischer, *Prog. Part. Nucl. Phys.* **62**, 549 (2009).
- [51] M. S. Bhagwat, A. Holl, A. Krassnigg, C. D. Roberts, and P. C. Tandy, *Phys. Rev. C* **70**, 035205 (2004).
- [52] M. Blank and A. Krassnigg, in preparation.